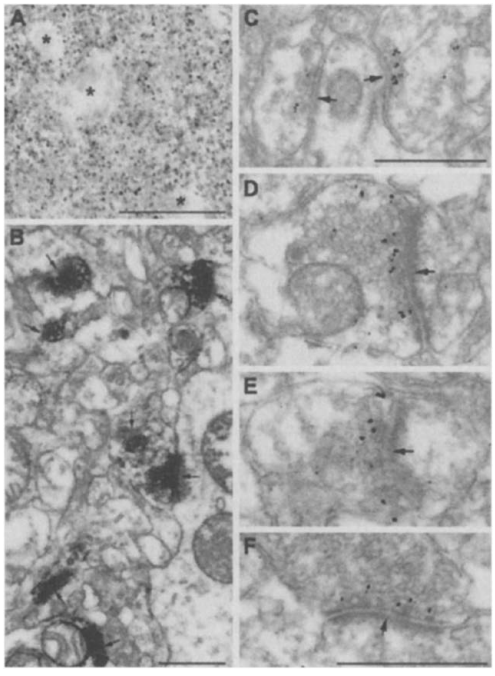

Fig. 3. Immunolocalization of neurotrypsin. Neurotrypsin was visualized in adult human cerebral cortex by using pre-embedding staining with a specific antibody against the proteolytic domain of neurotrypsin. (**A**) Immunohistochemical visualization of neurotrypsin with peroxidase-conjugated second antibody. The strong punctate immunolabeling of the neuropil is typical for a protein with synaptic localization. Neuronal somata (marked by asterisks) were unlabeled. (**B**) Preembedding immuno-EM localization by immunoperoxidase demonstrates the localization of neurotrypsin at presynaptic sites of axospinous and axodendritic asymmetric synapses in the cerebral cortex. The immunoperoxidase reaction product is associated with the presynaptic membrane and the active zone of the presynaptic terminal (arrows). (**C** to **F**) Immunogold localization of neurotrypsin at selected synapses. Note the exclusive labeling of presynaptic terminals in the region lining the synaptic cleft. Scale bars: (A), 100 μm; (B to F), 0.5 μm.

ample, both overexpression and inactivation of protease nexin-1, a serine protease inhibitor of the serpin family, altered hippocampal LTP (*31*). These data suggest that the balance between proteolytic enzymes and their inhibitors is crucial for the regulation of neural plasticity. In this context, neurotrypsin is an excellent candidate as a regulator of synaptic development and/or function, on the basis of its localization in presynaptic terminals; its strong expression in many brain areas during neural development; and its strong expression in adult brain, particularly in areas that are involved in learning and memory.

The results reported here emphasize the crucial role of synaptic proteolysis in higher brain function and open a novel field in the pathophysiology of mental retardation.

References and Notes

1. N. Roeleveld, G. A. Zielhuis, F. Gabreels, *Dev. Med. Child Neurol.* **39**, 125 (1997).
2. P. Stromme, *Dev. Med. Child Neurol.* **42**, 76 (2000).
3. J. Gezc *et al.*, *Nature Genet.* **13**, 105 (1996).
4. P. D'Adamo *et al.*, *Nature Genet.* **19**, 134 (1998).
5. P. Billuard *et al.*, *Nature* **392**, 923 (1998).
6. K. M. Allen *et al.*, *Nature Genet.* **20**, 25 (1998).
7. K. Merienne *et al.*, *Nature Genet.* **22**, 13 (1999).
8. A. Carrie *et al.*, *Nature Genet.* **23**, 25 (1999).
9. R. Zemni *et al.*, *Nature Genet.* **24**, 167 (2000).
10. K. Kutsche *et al.*, *Nature Genet.* **26**, 247 (2000).
11. I. Meloni *et al.*, *Nature Genet* **30**, 436 (2002).
12. T. Bienvenu *et al.*, *Hum. Mol. Genet.* **8**, 981 (2002).
13. W. Wu, A. Glinka, H. Delius, C. Niehrs, *Curr. Biol.* **10**, 1611 (2000).
14. Q. Lan, L. L. Niu, A. M. Fallon, *Biochim. Biophys. Acta* **1218**, 460 (1994).
15. N. Tiso *et al.*, *Biochem. Biophys. Res. Commun.* **225**, 983 (1996).
16. W. T. Tse *et al.*, *Genomics* **10**, 858 (1991).
17. R. M. Tombes, G. W. Krystal, *Biochim. Biophys. Acta* **1355**, 281 (1997).
18. X. Zhu *et al.*, *Cell* **85**, 661 (1996).
19. Y. Yamamura *et al.*, *Biochem. Biophys. Res. Commun.* **239**, 386 (1997).
20. T. P. Gschwend, S. R. Krueger, S. V. Kozlov, D. P. Wolfer, P. Sonderegger, *Mol. Cell. Neurosci.* **9**, 207 (1997).
21. D. P. Wolfer, R. Lang, P. Cinelli, R. Madani, P. Sonderegger, *Mol. Cell. Neurosci.* **18**, 407 (2001).
22. Materials and methods are available as supporting material on *Science* Online.
23. F. Molinari *et al.*, unpublished observations.
24. S. Yoshida, S. Shiosaka, *Int. J. Mol. Med.* **3**, 405 (1999).
25. Z. Qian, M. E. Gilbert, M. A. Colicos, E. R. Kandel, D. Kuhl, *Nature* **361**, 453 (1993).
26. N. W. Seeds, B. L. Williams, P. C. Bickford, *Science* **270**, 1992 (1995).
27. U. Frey, M. Muller, D. Kuhl, *J. Neurosci.* **16**, 2057 (1996).
28. Y. Y. Huang *et al.*, *Proc. Natl. Acad. Sci. U.S.A.* **93**, 699 (1996).
29. M. B. Gingrich, C. E. Junge P. Lynbostavsky, S. F. Traynelis, *J. Neurosci.* **20**, 4582 (2000).
30. A. Hirata *et al.*, *Cell. Neurosci.* **17**, 600 (2000).
31. A. Luthi *et al.*, *J. Neurosci.* **17**, 4688 (*1997*).

32. We wish to express our gratitude to the patients and their families for cooperation. We acknowledge the Centre National de Genotypage for its contribution to the genomewide screening, S. Audollent for technical assistance, and M. Salvador for helpful discussion. This study was supported in part by the Centre National de la Recherche Scientifique, the Fondation de France, a EURExpress grant, and the Swiss National Science Foundation.

Supporting Online Material

www.sciencemag.org/cgi/content/full/298/5599/1779/DC1

Materials and Methods

Fig. S1 to S3

References

27 July 2002; accepted 25 September 20002

Neurotoxicity and Neurodegeneration When PrP Accumulates in the Cytosol

Jiyan Ma,[1]* Robert Wollmann,[2] Susan Lindquist[3]†

Changes in prion protein (PrP) folding are associated with fatal neurodegenerative disorders, but the neurotoxic species is unknown. Like other proteins that traffic through the endoplasmic reticulum, misfolded PrP is retrograde transported to the cytosol for degradation by proteasomes. Accumulation of even small amounts of cytosolic PrP was strongly neurotoxic in cultured cells and transgenic mice. Mice developed normally but acquired severe ataxia, with cerebellar degeneration and gliosis. This establishes a mechanism for converting wild-type PrP to a highly neurotoxic species that is distinct from the self-propagating PrP^{Sc} isoform and suggests a potential common framework for seemingly diverse PrP neurodegenerative disorders.

Prion diseases are rare and inexorably fatal neurodegenerative disorders that can appear in sporadic, dominantly heritable, and transmissible forms (*1*). These diseases have unusually complex etiologies, and decades of research have failed to elucidate the pathogenic mechanism (*2–5*). Nonetheless, the prion protein PrP plays a pivotal role (*6*, *7*). A rare form of PrP with an altered protease-resistant conformation, PrP^{Sc}, is widely believed to be the infectious agent (or to constitute the major component of it) in transmissible forms of disease (*1*). But increasing evidence suggests that PrP^{Sc} is not itself neurotoxic. PrP^{Sc} is not observed in several inherited and experimentally induced forms of prion disease (*8–11*). And PrP knockout mice

[1]Howard Hughes Medical Institute, [2]Department of Pathology, University of Chicago, 5841 South Maryland Avenue, Chicago, IL 60637, USA. [3]Whitehead Institute for Biomedical Research, Massachusetts Institute of Technology, Nine Cambridge Center, Cambridge, MA 02142, USA.

*Present address: Department of Molecular and Cellular Biochemistry, Ohio State University, Columbus, OH 43210, USA.

†To whom correspondence should be addressed. E-mail: lindquist_admin@wi.mit.edu

are immune to the toxic effects of PrP^{Sc}, even when they receive high titers of PrP^{Sc} intracerebrally (*6*, *7*). Thus, neurotoxicity involves perturbations of endogenous PrP metabolism, but what perturbations might cause cell death remains a mystery.

PrP is a plasma membrane protein that begins its journey to the cell surface in the endoplasmic reticulum (ER). Like many proteins that traffic through the ER (*12*, *13*), a substantial fraction of PrP normally misfolds, is retrograde transported to the cytosol, and is degraded by proteasomes (*14*, *15*). Several PrP mutants that cause familial neurodegeneration are as stable as wild-type PrP once they mature (*16*, *17*), but are more likely to misfold during maturation (*18*), and in the one case tested, are more frequently subject to retrograde transport (*14*). In the cytosol, PrP is usually degraded so rapidly it is undetectable. However, when proteasome activity is compromised, PrP accumulates and sometimes converts to a PrP^{Sc}-like conformation (*19*). Proteasome inhibitors kill neuroblastoma cells more rapidly than other cultured cell types tested (*14*), yet the fraction of PrP that converts to a PrP^{Sc}-like form seems to have little influence on toxicity (*19*). Here we explore the relation between PrP misfolding, proteasome inhibition, accumulation of PrP in the cytosol, and neurotoxicity.

We first asked if the toxicity of proteasome inhibitors in neuroblastoma cells is related to the accumulation of PrP in their cytosol. We compared closely related lines, derived from murine N2A cells. WtPN2A cells were produced by transfection with a plasmid expressing wild-type PrP (wtPrP, amino acids 1 to 254) from a constitutive promoter (*20*). Bulk selection produced a pool of cells expressing PrP at different levels. By immunofluorescent staining and other analyses, we determined that the protein was localized at the surface in all cells (*21*). Cytosolic accumulation of PrP was induced by treatment with the reversible proteasome inhibitor MG132 (*22*) and confirmed by immunofluorescent staining (*21*).

Prior to proteasome inhibition, WtPN2A and N2A cultures were equally viable (*22*); during inhibition WtPN2A cells died much more rapidly (Fig. 1A and fig. S1). Seven days of regrowth in inhibitor-free medium were required to restore WtPN2A cultures to near confluence.

Before proteasome inhibition, PrP exhibited a normal heterogeneous pattern of glycosylation and fractionated in the supernatant after detergent lysis and centrifugation (Fig. 1B). Immediately after inhibition, much of the PrP fractionated in the pellet and migrated as expected for retrograde-transported PrP (*14*) (Fig. 1B), with its signal sequences removed, in a mostly unglycosylated form (*23*–*25*). After regrowth, PrP resumed its normal pattern of modification and localization. Although selection for the transgene was maintained continuously, cells that repopulated the culture produced much lower levels of PrP (Fig. 1B). A similar loss of PrP expression occurred with a variety of other proteasome inhibition-and-recovery protocols, including even very brief MG132 treatments (e.g., 3 hours) (*26*). Without the MG132 treatment, WtPN2A cells retained their original levels of PrP expression (Fig. 1B). Thus, cells with higher levels of PrP expression were selectively killed by treatment with the inhibitor.

In contrast, MG132 caused no selective killing in cells transfected with a plasmid encoding presenilin1, another membrane-associated protein that traffics through the ER and is subject to retrograde transport (*27*). When these cells were treated with the inhibitor, presenilin1 (like PrP) accumulated in the cytosol (*27*) in a detergent-insoluble form (Fig. 1C). However, the cells died at about the same rate as the parental N2A line (*26*), resumed growth rapidly when MG132 was removed (*26*), and retained high levels of presenilin expression after regrowth (Fig. 1C).

To address the importance of cytosolic localization of PrP in determining toxicity, we examined a line that had been clonally selected for high constitutive PrP expression, moPrP (*28*). The PrP protein produced by these cells had an altered pattern of glycosylation (Fig. 1D), suggesting it was subject to a

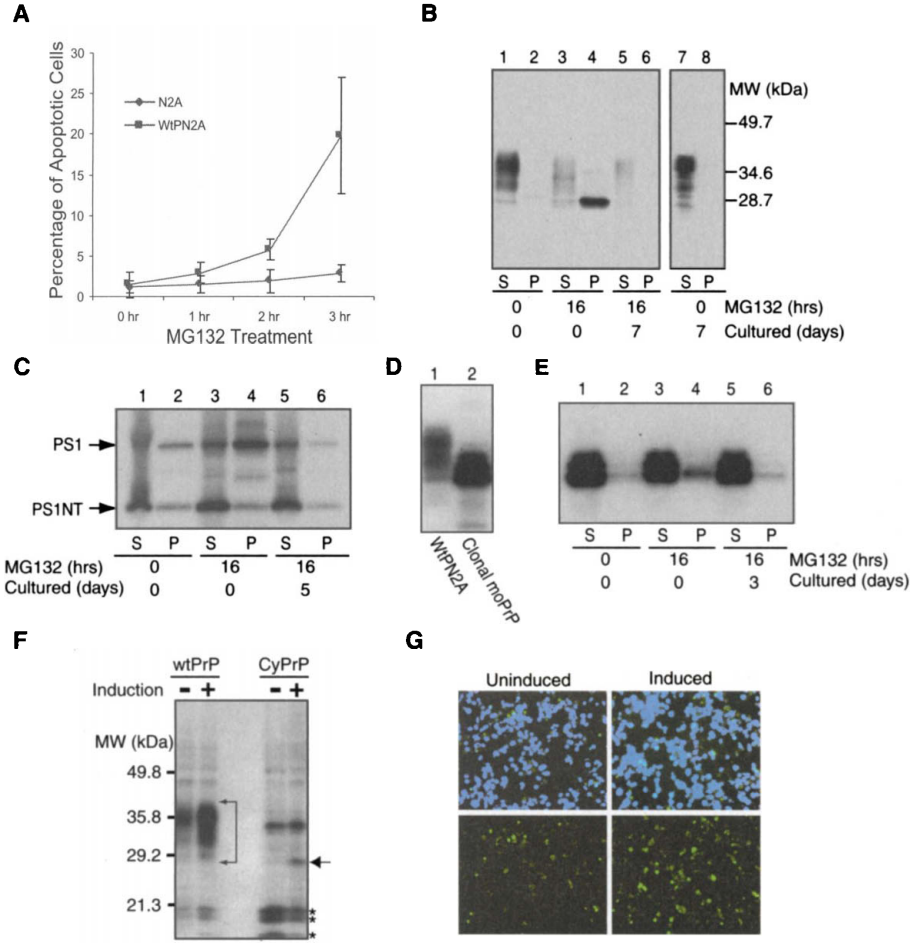

Fig. 1. Toxicity of cytosolic PrP. (**A**) N2A cells and WtPN2A cells were treated with MG132 for various times as indicated; apoptotic cells were identified by the TUNEL assay. (**B**) WtPN2A cells treated with or without MG132 for 16 hours were either harvested immediately or cultured to confluence (7 days). PrP in the supernatant (s) and pellet (p) fractions of cell lysates was detected. (**C**) N2A cells stably transfected with presenilin1 (PS1) were treated as in (A). Arrows indicate full-length PS1, or an NH_2-terminal fragment, PS1NT. (**D**) Different modification states of PrP in WtPN2A and moPrP cells detected as differences in electrophoretic mobility. (**E**) moPrP cells were treated as in (A). (**F**) Immunoblot detection of PrP in N2A cells stably expressing ecdysone-inducible wtPrP or cyPrP. Arrows, PrP; asterisks, specific PrP cleavage products. (**G**) N2A cells stably expressing ecdysone-inducible cyPrP before and after induction. Apoptotic cells are green (TUNEL assay) and nuclei are blue (DAPI , 4′,6-diamidino-2-phenylindole). PS1 and PrP were detected by immunoblot analysis with antibodies specific for PS1 or PrP (3F4). Coomassie staining demonstrated equal loading of all supernatant and all pellet fractions except that lanes 3 and 4 of (B) were slightly underloaded.

different pattern of intracellular trafficking (*29*). Indeed, when moPrP cells were treated with MG132, little PrP aggregated and by immunofluorescent staining none was accumulated in the cytosol (Fig. 1E) (*26*). Although these cells expressed PrP at a very high level, they retained viability in the presence of MG132 even better than parental N2A cells (*30*), returned to confluence very quickly, and retained their high levels of PrP expression (Fig. 1E).

Finally, we asked if increasing the appearance of PrP in the cytosol was sufficient to kill cells in the absence of proteasome inhibitors. We compared murine fibroblast–derived NIH3T3 cells with neuroblastoma cells. Each cell line was separately transfected with wtPrP and with a cytosolic form (cyPrP, amino acids 23 to 230), which precisely eliminated the NH_2-terminal and the COOH-terminal sequences that are cleaved upon ER entry. CyPrP has no cryptic ER translocation signals (*31*) and is unglycosylated, as is most retrograde-transported PrP (*14*) (Fig. 1B). Using a constitutive promoter (*20*), we readily established stable lines from NIH3T3 cells with both wtPrP and cyPrP (*26*). As expected, much less cyPrP accumulated than wtPrP because cyPrP was exposed to proteasomes directly after synthesis. Successful transfection and expression were confirmed by rapid accumulation of cyPrP upon addition of proteasome inhibitors (*26*). With neuroblastoma cells, stable lines were readily established with wtPrP, but could not be established with cyPrP, despite many attempts. Thus, cytosolic PrP appears to be toxic, but in a cell type–dependent manner.

For better transgene manipulation in neuroblastoma cells, we expressed wtPrP and cyPrP from an ecdysone-inducible promoter. Again, stable lines were readily established with wtPrP (Fig. 1F). Constitutive expression of wtPrP was higher than expected with this tightly controlled promoter (*32*), perhaps because the PrP coding sequence contains an enhancer for expression in this cell type (Fig. 1F). With this inducible promoter, lines could be established with cyPrP, but they grew very slowly. (This was likely due to leaky expression of the transgene, because stable lines were readily established with unrelated constructs.) Immunofluorescence staining of cyPrP was faint but clearly above background (*26*). By immunoblotting, full-length cyPrP did not accumulate in quantities sufficient for detection, but specific cleavage fragments from the transgene did accumulate (Fig. 1F). Unlike cells transfected with wtPrP, cells transfected with cyPrP continuously yielded high levels of TUNEL (terminal deoxynucleotidyl transferase–mediated dUTP nick-end labeling)-positive cells, indicating that even small amounts of cytosolic PrP, or perhaps its cleavage products, are toxic in neuroblastoma cells (Fig. 1G). When expression was induced with ecdysone overnight, the number of TUNEL-positive cells doubled (from 6 to 14%; Fig. 1G), confirming the extreme toxicity of cyPrP.

To test if cytosolic PrP was toxic in a manner relevant to disease in whole animals, we created transgenic mice expressing cyPrP from a commonly used PrP promoter (*33*, *34*). Three founder mice carrying the transgene were identified by genomic polymerase chain reaction (table S1). One did not breed, developed hind limb paresis after 6 months, and died 4.5 months later. The other founders produced many transgenic progeny, all of which exhibited pathology that was very different from that of transgenic mice neurologically impaired for other reasons, but very similar to that of transgenic mice producing mutant forms of PrP (*34*–*36*).

One founder, 2D1, exhibited no phenotype itself, but all of its transgenic offspring began to show an unsteady gait at 29 days (±2 days). Thereafter, they grew more slowly than wild-type siblings (*37*). At 7 weeks, they were severely ataxic, very slow to respond to external stimuli, and showed tail rigidity (Fig. 2 and fig. S2; table S1 and Movie S1). At 10 to 11 weeks, when death was obviously imminent as determined by the veterinarian, mice were euthanized.

Founder 1D4 and its transgenic progeny developed disheveled hair and frequent scratching at 5 to 12 months of age. Mild ataxia and weight loss appeared several weeks later (Fig. 2, table S1, and Movie S2). F_2 progeny carrying two copies of the transgene (fig. S6) developed pathology with a much faster onset (~2 months) and extreme neurodegeneration, demonstrating a dosage relation between cyPrP and the pace of pathogenesis (Movie S3) (*26*).

Upon dissection, the only overt sign of disease in 2D1 and 1D4 mice was cerebellar atrophy (fig. S3). Histology revealed very similar cerebellar pathology with a timing and severity that corresponded to the onset and progression of ataxia. Massive neuronal loss occurred in the granular layer, and the molecular layer was also affected (Fig. 3) (*22*, *36*). Notably, Purkinje neurons, located between the molecular and granular layers, were unaffected. Purkinje cells are not spared in natural forms of prion diseases; however, the PrP promoter we used lacked an enhancer element required for expression in this cell type (*35*, *38*). Thus, pathology was cell autonomous and related to transgene expression.

Severe gliosis, characteristic of prion diseases, was revealed by immunohistochemical staining with an antibody against glial fibrillary acidic protein (GFAP) in both 2D1 and 1D4 mice (Fig. 3A) (*26*). At early stages, behavior, brain morphologies, and the timing of granular neuron migration were indistinguishable in transgenic and wild-type littermates (Fig. 3B and fig. S4). Therefore, pathology was due to degeneration rather than to problems in development.

PrP is widely expressed, but prion disease pathologies are generally restricted to the central nervous system (*1*). As expected (*1*), using a ribonuclease protection assay (*22*), we found that endogenous PrP was expressed at high levels in the brain and at modest levels in heart and skeletal muscle (Fig. 4A and fig. S7). In 2D1 mice, transgene expression was similar to endogenous PrP expression in the brain and slightly higher in heart and muscle (Fig. 4A, fig. S7, and table S1). Thus, the extreme pathology in the brains of transgenic mice and the absence of detectable pathology in heart and muscle recapitulated the tissue selectivity of prion disease.

Three PrP species were detected in wild-type brains (Fig. 4B): the characteristically abundant monoglycosylated and diglycosylated forms and the less abundant unglycosylated form (*39*). CyPrP migrates at the same position as the smallest form of endogenous PrP. Because cytosolic PrP is directly subject to proteasomal degradation, we did not expect substantial accumulation of cyPrP. Quantification revealed only a twofold increase in the smallest (27 kD) PrP band in 2D1 mice in three of three 2D1 brain samples examined (Fig. 4B) (*26*). Against the reduced endogenous PrP background in the heart, cyPrP was readily detected by increased reactivity of the 27-kD species (Fig. 4C) (*26*). In 1D4 mice, transgene RNA was detected at a lower level, and the protein could not be detected reliably above background (table S1) (*26*).

The conformation of PrP associated with infectious PrP diseases, PrP^{Sc}, is detergent insoluble and yields a characteristic resistant fragment after cleavage by proteinase K (*1*). No PrP^{Sc}, nor any other forms of aggregated

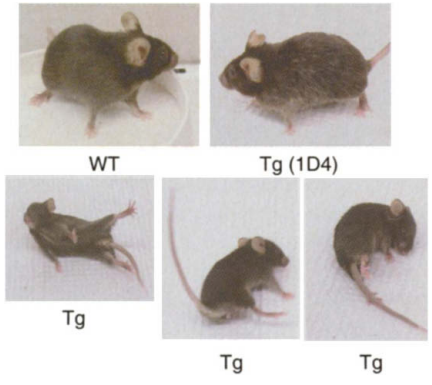

Fig. 2. CyPrP transgenic mice exhibit ataxia and hair phenotypes. Photographs of wild-type mouse (upper left panel), 1D4 transgenic mouse showing hair phenotype (upper right panel), and 2D1 transgenic mice showing ataxia (lower panels).

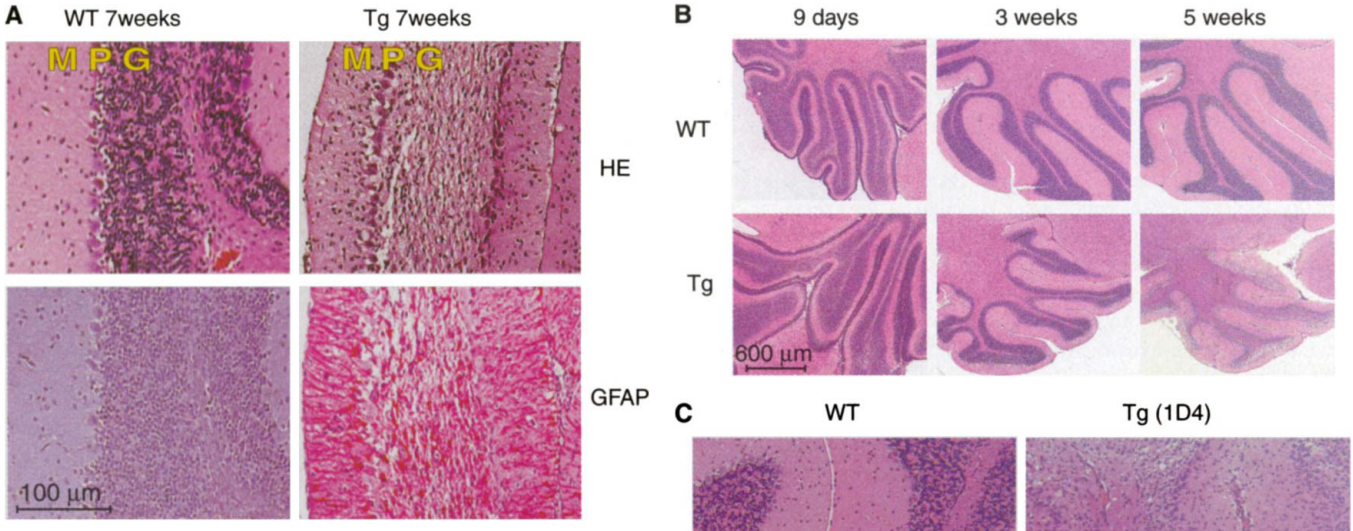

Fig. 3. Neuropathology of transgenic mice. (**A**) (Top) Hemotoxylin and eosin (HE) staining of cerebella of 7-week-old wild-type and transgenic 2D1 littermates. M, molecular layer; P, Purkinje cells; G, granular layer. (Bottom) GFAP immunostaining (red) of adjacent sections with hemotoxylin counterstaining (blue). (**B**) HE staining of cerebella of wild-type and transgenic 2D1 littermates from 9 days to 5 weeks old. (**C**) HE staining of cerebella of wild-type and transgenic 1D4 littermates.

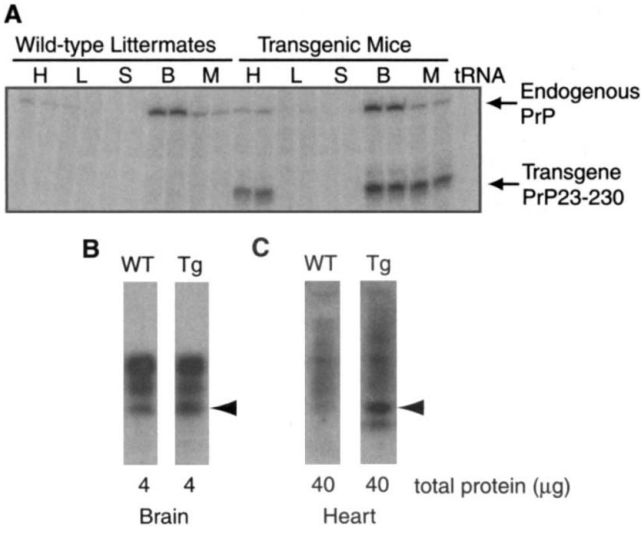

Fig. 4. Expression of transgene. (**A**) RNA expression for endogenous PrP and transgene (PrP23-230) in different tissues of two pairs of wild-type and transgenic littermates. H, heart; L, liver; S, spleen; B, brain; M, skeletal muscle. (**B** and **C**) Immunoblot analysis of PrP expression in brain (B) and heart (C). Arrow indicates the migration position of cyPrP.

PrP, could be detected in 2D1 or 1D4 animals at any of several stages tested (*26*, *36*). As a positive control, we readily detected PrP^{Sc} in brain samples from infected hamster. The absence of pathology in Purkinje cells also attested to the absence of PrP^{Sc}; neurons immediately adjacent to Purkinje cells were subject to massive degeneration, and an infectious agent would have been expected to spread to them.

This work, together with our earlier study (*14*), establishes a mechanism by which wild-type PrP can be converted into a highly neurotoxic species. Misfolded PrP molecules are retrograde transported to the cytosol for degradation by the proteasome (*14*, *15*). The remarkable efficiency of proteasomal degradation normally prevents toxic species from accumulating, but when the proteasome's ability to degrade PrP is compromised, as might naturally occur with stress and aging, the increase in cytosolic PrP would kill the neuron. Depending upon the rate of misfolding and retrograde transport, the same mechanism might lead to the production of PrP^{Sc} (*19*), but this is not the toxic species. Very small quantities of soluble PrP are toxic, perhaps acting directly or through PrP cleavage products (produced by caspases or other specific mechanisms) to signal cell death pathways. Indeed, the toxicity of cytosolic PrP is so extreme as to suggest it is an evolved mechanism to kill neurons with PrP folding problems, thereby reducing the risk that PrP will accumulate at sufficient levels to produce the disseminating PrP^{Sc} form.

Our results suggest a unifying model for PrP-associated diseases that would otherwise appear to have disparate etiologies. Mutations associated with neurodegeneration are distributed throughout the PrP coding sequence (*1*), and these proteins have been reported to accumulate in different compartments and perturb metabolism in a variety of ways (*18*, *40*–*42*). While accepting that these differences may modify disease progression, it seems simpler to postulate that a common mechanism underlies toxicity: The mutations increase misfolding of PrP, recognition by the cellular quality-control systems, and transport to the cytosol. Such a mechanism can also explain pathogenesis in infectious prion diseases, if PrP^{Sc} induces perturbations in the folding and trafficking of endogenous PrP (*19*). In all of these cases, the low levels of soluble PrP required for toxicity would hitherto have eluded detection. This model would also resolve controversies about why some PrP mutations generate PrP^{Sc} and others do not (*4*, *10*, *11*, *43*, *44*). Cytosolic conversion of PrP depends on its rate of appearance in the cytosol (*19*) and may also be influenced in that compartment by the nature of the mutation (*45*).

Our work has implications for the use of proteasome inhibitors in biomedical research and as therapeutic agents (*46*, *47*). Because small quantities of cytosolic PrP can cause severe neurodegeneration and because interfering with proteasome degradation leads to the accumulation of cytosolic PrP, proteasome inhibitors should be handled with caution, with strong preference given to inhibitors that do not cross the blood-brain barrier.

Finally, alterations in PrP trafficking, such as that observed here with moPrP cells (*48–50*), can prevent toxic accumulation of PrP in the cytosol without compromising viability. This provides a potential therapeutic strategy for prion disease.

References and Notes

1. S. B. Prusiner, *Proc. Natl. Acad. Sci. U.S.A.* **95**, 13363 (1998).
2. B. Caughey, B. Chesebro, *Trends Cell Biol.* **7**, 56 (1997).
3. R. Chiesa, D. A. Harris, *Neurobiol. Dis.* **8**, 743 (2001).
4. A. Aguzzi, F. L. Heppner, *Cell Death Differ.* **7**, 889 (2000).
5. J. Collinge, *Annu. Rev. Neurosci.* **24**, 519 (2001).
6. H. Bueler *et al.*, *Cell* **73**, 1339 (1993).
7. S. Brandner *et al.*, *Nature* **379**, 339 (1996).
8. K. K. Hsiao *et al.*, *Proc. Natl. Acad. Sci. U.S.A.* **91**, 9126 (1994).
9. C. I. Lasmezas *et al.*, *Science* **275**, 402 (1997).
10. T. Kitamoto, R. Iizuka, J. Tateishi, *Biochem. Biophys. Res. Commun.* **192**, 525 (1993).
11. F. Tagliavini *et al.*, *Cell* **79**, 695 (1994).
12. R. R. Kopito, *Cell* **88**, 427 (1997).
13. S. W. Fewell, K. J. Travers, J. S. Weissman, J. L. Brodsky, *Annu. Rev. Genet.* **35**, 149 (2001).
14. J. Ma, S. Lindquist, *Proc. Natl. Acad. Sci. U.S.A.* **98**, 14955 (2001).
15. Y. Yedidia, L. Horonchik, S. Tzaban, A. Yanai, A. Taraboulos, *EMBO J.* **20**, 5383 (2001).
16. W. Swietnicki, R. B. Petersen, P. Gambetti, W. K. Surewicz, *J. Biol. Chem.* **273**, 31048 (1998).
17. S. Liemann, R. Glockshuber, *Biochemistry* **38**, 3258 (1999).
18. L. Ivanova, S. Barmada, T. Kummer, D. A. Harris, *J. Biol. Chem.* **276**, 42409 (2001).
19. J. Ma, S. Lindquist, *Science* **298**, 1785 (2002); published online 17 October 2002 (10.1126/science.1073619).
20. Cytomegalovirus promoter.
21. Experiments were performed as in (*14*).
22. Materials and methods are available as supporting materials on *Science* Online.
23. First, unglycosylated proteins are more likely to misfold in the ER and be subject to retrograde transport; second, glycosylated species that are retrograde transported are subject to cytoplasmic deglycosidases.
24. A. J. Parodi, *Annu. Rev. Biochem.* **69**, 69 (2000).
25. T. Suzuki, H. Park, N. M. Hollingsworth, R. Sternglanz, W. J. Lennarz, *J. Cell Biol.* **149**, 1039 (2000).
26. J. Ma, R. Wollmann, S. Lindquist, data not shown.
27. J. A. Johnston, C. L. Ward, R. R. Kopito, *J. Cell Biol.* **143**, 1883 (1998).
28. B. Chesebro *et al.*, *Dev. Biol. Stand.* **80**, 131 (1993).
29. A. Helenius, M. Aebi, *Science* **291**, 2364 (2001).
30. More than 50% of N2A cells died within 12 hours of proteasome treatment, but less than 5% of moPrP cells died during the same period.
31. C. Holscher, U. C. Bach, B. Dobberstein, *J. Biol. Chem.* **276**, 13388 (2001).
32. D. No, T. P. Yao, R. M. Evans, *Proc. Natl. Acad. Sci. U.S.A.* **93**, 3346 (1996).
33. D. R. Borchelt *et al.*, *Genet. Anal.* **13**, 159 (1996).
34. R. Chiesa, P. Piccardo, B. Ghetti, D. A. Harris, *Neuron* **21**, 1339 (1998).
35. D. Shmerling *et al.*, *Cell* **93**, 203 (1998).
36. Supporting text and data are available on *Science* Online.
37. Slow growth might be due to ataxia-associated problems with eating and drinking, although special care was taken to provide accessible food and water.
38. R. Chiesa *et al.*, *Proc. Natl. Acad. Sci. U.S.A.* **97**, 5574 (2000).
39. M. Russelakis-Carneiro, G. P. Saborio, L. Anderes, C. Soto, *J. Biol. Chem.* **18**, 18 (2002).
40. H. Lorenz, O. Windl, H. A. Kretzschmar, *J. Biol. Chem.* **277**, 8508 (2002).
41. N. Singh *et al.*, *J. Biol. Chem.* **272**, 28461 (1997).
42. G. Zanusso *et al.*, *J. Biol. Chem.* **274**, 23396 (1999).
43. D. Doyle, M. Rogers, *Trends Genet.* **14**, 171 (1998).
44. P. Piccardo *et al.*, *J. Neuropathol. Exp. Neurol.* **57**, 979 (1998).
45. J. J. Liu, S. Lindquist, *Nature* **400**, 573 (1999).
46. J. Adams, V. J. Palombella, P. J. Elliott, *Invest. New Drugs* **18**, 109 (2000).
47. P. Andre *et al.*, *Proc. Natl. Acad. Sci. U.S.A.* **95**, 13120 (1998).
48. In a related manner, our model explains the puzzling ability of certain neuroblastoma lines to continuously produce PrP^{Sc} without dying. In these cells, PrP^{Sc} conversion appears to occur solely on the cell surface and in endocytic compartments.
49. B. Caughey, G. J. Raymond, *J. Biol. Chem.* **266**, 18217 (1991).
50. K. Doh-Ura, T. Iwaki, B. Caughey, *J. Virol.* **74**, 4894 (2000).

51. We thank B. Caughey, G. Thinakaran, and J. Tatzelt for providing cell lines and antibodies; X. Wang, Y. Wang, and E. Rehm for technical help; members of the Lindquist lab for critical reading of this manuscript; and NIH (GM25874) and the Howard Hughes Medical Institute for funding this research. This work was initiated in S.L.'s laboratory at the University of Chicago and continued there under her supervision after her move to the Whitehead Institute for Biomedical Research.

Supporting Online Material

www.sciencemag.org/cgi/content/full/1073725/DC1
Materials and Methods
SOM Text
Figs. S1 to S7
Table S1
Movies S1 to S3

8 May 2002; accepted 30 September 2002
Published online 17 October 2002;
10.1126/science.1073725
Include this information when citing this paper.

Conversion of PrP to a Self-Perpetuating PrP^{Sc}-like Conformation in the Cytosol

Jiyan Ma[1]* and Susan Lindquist[2]†

A rare conformation of the prion protein, PrP^{Sc}, is found only in mammals with transmissible prion diseases and represents either the infectious agent itself or a major component of it. The mechanism for initiating PrP^{Sc} formation is unknown. We report that PrP retrogradely transported out of the endoplasmic reticulum produced both amorphous aggregates and a PrP^{Sc}-like conformation in the cytosol. The distribution between these forms correlated with the rate of appearance in the cytosol. Once conversion to the PrP^{Sc}-like conformation occurred, it was sustained. Thus, PrP has an inherent capacity to promote its own conformational conversion in mammalian cells. These observations might explain the origin of PrP^{Sc}.

Changes in the trafficking and conformation of the mammalian prion protein (PrP) are associated with a group of fatal neurodegenerative diseases (*1*). Some PrP-associated diseases involve an infectious agent hypothesized to be an altered conformation of PrP known as PrP^{Sc}. PrP^{Sc} is thought to propagate by converting other PrP molecules to the same conformation (*1*). Alternatively, PrP^{Sc} may propagate by association with an as-yet-unidentified infectious agent (*2, 3*). In either case, conversion of PrP to PrP^{Sc} is a central event in the etiology of transmissible PrP-associated diseases, yet the mechanism that initiates conversion is a complete mystery.

When PrP is expressed in the cytosol of yeast cells, a fraction converts to a form with the biochemical properties of PrP^{Sc}. This might be an aberration of heterologous expression. Alternatively, some general features of the cytosol (e.g., chaperones, the reducing environment) may promote conversion (*4*). A natural route by which PrP enters the cytosol of mammalian cells is retrograde transport (*5, 6*), which delivers proteins that misfold during maturation in the endoplasmic reticulum (ER) to the cytosol for degradation by proteasomes (*7, 8*). When proteasome activity is blocked, PrP accumulates in the cytosol (*5*). If the number of PrP molecules delivered to the cytosol ever exceeds its quality-control capacity, some PrP might convert to a PrP^{Sc} form.

Spontaneous prion diseases are very rare. Even in individuals with the most virulent PrP mutations, several decades elapse before chance and circumstance produce conversion. We increased the likelihood of detecting conversion events by assessing the conformational state of the PrP that accumulated in the cytosol when proteasome activity was compromised (Fig. 1) (*9*). Several cell types were transfected with a wild-type mouse PrP gene (*10*), treated with one of three different proteasome inhibitors, lysed with detergents, and subjected to centrifugation (*10*).

An increase in PrP accumulation was

[1]Howard Hughes Medical Institute (HHMI), University of Chicago, Chicago, IL 60637, USA. [2]Whitehead Institute for Biomedical Research, Massachusetts Institute of Technology, 9 Cambridge Center, Cambridge, MA 02142, USA.

*Present address: Department of Molecular and Cellular Biochemistry, Ohio State University, Columbus, OH 43210, USA.

†To whom correspondence should be addressed. E-mail: lindquist_admin@wi.mit.edu